Available online at www.sciencedirect.com

ScienceDirect

Nuclear Physics B 896 (2015) 200–211

NUCLEAR PHYSICS B

www.elsevier.com/locate/nuclphysb

Higgs boson production and decay at e^+e^- colliders as a probe of the Left–Right twin Higgs model

Jinzhong Han [a,*], Shaofeng Li [a], Bingfang Yang [b,c,*], Ning Liu [b,*]

[a] *School of Physics and Electromechanical Engineering, Zhoukou Normal University, Henan, 466001, China*
[b] *College of Physics and Electronic Engineering, Henan Normal University, Xinxiang 453007, China*
[c] *School of Materials Science and Engineering, Henan Polytechnic University, Jiaozuo 454000, China*

Received 26 January 2015; received in revised form 5 April 2015; accepted 19 April 2015

Available online 23 April 2015

Editor: Hong-Jian He

Abstract

In the framework of the Left–Right twin Higgs (LRTH) model, we consider the constrains from the latest search for high-mass dilepton resonances at the LHC and find that the heavy neutral boson Z_H is excluded with mass below 2.76 TeV. Under these constrains, we study the Higgs–Gauge coupling production processes $e^+e^- \to ZH$, $e^+e^- \to \nu_e\bar{\nu}_e H$ and $e^+e^- \to e^+e^- H$, top quark Yukawa coupling production process $e^+e^- \to t\bar{t}H$, Higgs self-couplings production processes $e^+e^- \to ZHH$ and $e^+e^- \to \nu_e\bar{\nu}_e HH$ at e^+e^- colliders. Besides, we study the major decay modes of the Higgs boson, namely $h \to f\bar{f}(f = b, c, \tau)$, $VV^*(V = W, Z)$, gg, $\gamma\gamma$. We find that the LRTH effects are sizable so that the Higgs boson processes at e^+e^- collider can be a sensitive probe for the LRTH model.

1. Introduction

The hunt for Higgs bosons is one of the most important goals at the Large Hadron Collider (LHC). On the 4th of July 2012, CERN announced that both the ATLAS [1] and CMS [2] exper-

* Corresponding authors.
E-mail addresses: hanjinzhong@zknu.edu.cn (J. Han), yangbingfang@htc.edu.cn (B. Yang), wlln@mail.ustc.edu.cn (N. Liu).

http://dx.doi.org/10.1016/j.nuclphysb.2015.04.018

iments presented very strong evidence for a new Higgs-like boson with mass around 125 GeV. With the growingly accumulated date, the properties of this particle are consistent with those of Higgs boson predicted by the Standard Model (SM) [3,4]. Though the LHC offers obvious advantages in proving very high energy and very large rates in typical reactions, the measuring precision will be restricted due to the complicated background. However, the most precise measurements will be performed in the clean environment of the future e^+e^- colliders, like the International Linear Collider (ILC) [5].

It is well known, the main production processes of the Higgs boson in e^+e^- collisions are the Higgs-strahlung process $e^+e^- \to ZH$ and the WW fusion process $e^+e^- \to \nu_e\bar{\nu}_e H$. The cross section for the Higgs-strahlung process is dominant at the low energy. For $\sqrt{s} \geq 500$ GeV, the cross section for the WW fusion is dominant. The cross section for the ZZ fusion process $e^+e^- \to e^+e^-H$ increases significantly with the center-of-mass (c.m.) energy increasing, and can exceed that of ZH production around 1 TeV. These three processes can be well used to test the Higgs–Gauge couplings.

The large top quark Yukawa coupling is speculated to be sensitive to new physics, it can be studied through the associated production of Higgs boson with top quark pairs $e^+e^- \to t\bar{t}H$ at the ILC. This study will play an important role for precision measurements of the top quark Yukawa coupling. In addition, the Higgs self-coupling is the key ingredient of the Higgs potential and their measurement is indispensable for understanding the electroweak symmetry breaking. The Higgs self-coupling can be studied through the double Higgs boson production processes $e^+e^- \to ZHH$ and $e^+e^- \to \nu_e\bar{\nu}_e HH$ at the ILC. And many relevant works mentioned above have been extensively studied in the context of the SM [6] and some new physics models [7–9].

As an extension of the SM, the Left–Right twin Higgs (LRTH) model has been proposed as an alternative solution to the little hierarchy problem [10,11]. The idea of twin Higgs similar to that of little Higgs, in that the SM-like Higgs emerges as a pseudo-Goldstone boson [12]. The twin Higgs mechanism can be implemented in LRTH model with the discrete symmetry being identified with left–right symmetry. The phenomenology of the LRTH model has been studied in Refs. [13–17]. In the LRTH model, some new particles are predicted and some SM couplings are modified so that the Higgs properties may deviate from the SM Higgs boson. So the Higgs boson processes are ideal ways to probe the LRTH model at the e^+e^- colliders. In this paper, we mainly study the Higgs boson production processes $e^+e^- \to ZH$, $e^+e^- \to \nu_e\bar{\nu}_e H$, $e^+e^- \to e^+e^-H$, $e^+e^- \to t\bar{t}H$, $e^+e^- \to ZHH$ and $e^+e^- \to \nu_e\bar{\nu}_e HH$. Besides, we consider the major decay modes of the Higgs boson $h \to f\bar{f}(f = b, c, \tau)$, $VV^*(V = W, Z)$, gg, $\gamma\gamma$ in the LRTH model.

The paper is organized as follows. In Section 2 we briefly review the basic content of the LRTH model related to our work. In Section 3 and Section 4 we respectively investigate the Higgs boson production and decay processes, and give the numerical results and discussions. Finally, we give a short conclusion in Section 5.

2. A brief review of the LRTH model

Here we will briefly review the ingredients which are relevant to our calculations, and a detailed description of the LRTH model can be found in Ref. [13]. The LRTH model introduces the heavy gauge bosons $W_H^{\pm}$ and Z_H, the extra Higgs bosons ϕ^0 and $\phi^{\pm}$, and the top quark partner T. The masses of theses particles are given by:

$$M_{W_H}^2 = \frac{1}{2}g^2(\hat{f}^2 + f^2\cos^2 x), \tag{1}$$

$$M_{Z_H}^2 = \frac{g^2 + g'^2}{g^2}(M_W^2 + M_{W_H}^2) - M_Z^2, \tag{2}$$

$$m_{\phi^0}^2 = \frac{\mu_r^2 f \hat{f}}{\hat{f}^2 + f^2 \cos^2 x}\left\{\frac{\hat{f}^2\left[\cos x + \frac{\sin x}{x}(3+x^2)\right]}{f^2\left(\cos x + \frac{\sin x}{x}\right)^2} + 2\cos x + \frac{f^2\cos^2 x(1+\cos x)}{2\hat{f}^2}\right\}, \tag{3}$$

$$M_T^2 = \frac{1}{2}(M^2 + y^2 f^2 + N_t), \tag{4}$$

where $g = e/S_W$, $g' = e/\sqrt{\cos 2\theta_W}$, $S_W = \sin\theta_W$, θ_W is the Weinberg angle, $x = v/(\sqrt{2}f)$ with v is the electroweak scale, $N_t = \sqrt{(y^2 f^2 + M^2)^2 - y^4 f^4 \sin^2 2x}$ and the mass parameter M is the mixing between the SM top quark and its partner T. The Higgs vacuum expectation values (VEVs) f, $\hat{f}$ will be bounded by electroweak precision measurements. If we set $v = 246$ GeV, f and $\hat{f}$ will be interconnected. In addition, the top Yukawa coupling will also be of order one if $M_T \leq f$ and the parameter y is of order one. The expression forms of the couplings related to our calculations are given as follows [13,18]:

$$g_L^{t\bar{T}Z} = \frac{eC_L S_L}{2C_W S_W}, \qquad g_R^{t\bar{T}Z} = \frac{ef^2 x^2 S_W C_R S_R}{2\hat{f}^2 C_W^3}; \tag{5}$$

$$g_L^{t\bar{T}Z_H} = \frac{eC_L S_L S_W}{2C_W\sqrt{\cos 2\theta_W}}, \quad g_R^{t\bar{T}Z_H} = -\frac{eC_R S_R C_W}{2S_W\sqrt{\cos 2\theta_W}}; \tag{6}$$

$$g_L^{Z_H e^+ e^-} = \frac{eS_W}{2C_W\sqrt{\cos 2\theta_W}}, \quad g_R^{Z_H e^+ e^-} = \frac{e(1-3\cos 2\theta_W)}{4S_W C_W\sqrt{\cos 2\theta_W}}; \tag{7}$$

$$V_{Z\bar{\nu}_e\nu_e} = \frac{e\gamma_\mu P_L}{2C_W S_W}, \qquad V_{Z_H\bar{\nu}_e\nu_e} = \frac{eS_W\gamma_\mu P_L}{2C_W\cos 2\theta_W}; \tag{8}$$

$$V_{Z_{H\mu}Z_{H\nu}H} = -\frac{e^2 fx}{\sqrt{2}C_W^2 S_W^2}g_{\mu\nu}, \quad V_{Z_\mu Z_{H_\nu}H} = \frac{e^2 fx}{\sqrt{2}C_W^2\sqrt{\cos 2\theta_W}}g_{\mu\nu}; \tag{9}$$

$$V_{t\bar{t}\phi^0} = -\frac{iy}{\sqrt{2}}S_L S_R, \qquad V_{t\bar{t}H} = -\frac{em_t C_L C_R}{2m_W S_W}; \tag{10}$$

$$V_{t\bar{T}H} = -\frac{y}{\sqrt{2}}[(C_L S_R + S_L C_R x)P_L + (C_L S_R x + S_L C_R)P_R]; \tag{11}$$

$$V_{\phi^0 Z_\mu H} = \frac{iexp3_\mu}{6S_W C_W}, \qquad V_{\phi^0 Z_{H\mu}H} = \frac{iex[(14-17S_W^2)p2_\mu - (4-S_W^2 p1_\mu)]}{18S_W C_W\cos 2\theta_W}; \tag{12}$$

$$V_{Z_\mu Z_{H_\nu}HH} = \frac{e^2}{C_W^2\cos 2\theta_W}g_{\mu\nu}, \quad V_{Z_{H\mu}Z_{H\nu}HH} = -\frac{e^2}{C_W^2 S_W^2}g_{\mu\nu}; \tag{13}$$

where

$$S_L = \frac{1}{\sqrt{2}}\sqrt{1 - (y^2 f^2\cos 2x + M^2)/N_t}, \quad C_L = \sqrt{1 - S_L^2}; \tag{14}$$

$$S_R = \frac{1}{\sqrt{2}}\sqrt{1 - (y^2 f^2\cos 2x - M^2)/N_t}, \quad C_R = \sqrt{1 - S_R^2}. \tag{15}$$

Table 1
The masses (in GeV) of m_T, m_{Z_H} and m_{ϕ^0} used in this paper.

f (GeV)	800	900	1000	1100	1200	1300	1400	1500
$m_T(M=0)$	783.1	885.5	987.5	1089.2	1190.7	1291.9	1393.0	1494.0
$m_T(M=150)$	809.8	908.5	1007.4	1106.6	1206.0	1305.4	1404.9	1504.5
$m_{Z_H}(M=0)$	2307.9	2676.3	3038.5	3396.0	3750.0	4100.9	4449.6	4796.4
$m_{Z_H}(M=150)$	2403.0	2761.3	3115.1	3465.5	3813.3	4159.1	4503.2	4845.9
$m_{\phi^0}(M=0)$	113.4	115.2	116.4	117.4	118.1	118.7	119.2	119.5
$m_{\phi^0}(M=150)$	115.7	117.0	117.9	118.6	119.2	119.6	119.9	120.2

3. Higgs productions in the LRTH model at e^+e^- colliders

In this section, we will study the contributions of the LRTH model to three different types of Higgs boson production processes at e^+e^- colliders separately. In our calculations, the SM input parameters are taken from Ref. [19]. We take the SM-like Higgs mass as $m_H = 125$ GeV. The LRTH parameters involved in the amplitudes are the breaking scale f, the masses m_T, m_{Z_H}, m_{ϕ^0} and the mixing parameter M. The masses m_T, m_{Z_H} and m_{ϕ^0} are correlated to f and M, and parts of their values are listed in Table 1. The value of the mixing parameter M is constrained by the $Z \to b\bar{b}$ branching ratio and oblique parameters [13]. In our analysis, we take small M and pick two typical values of $M = 0$ and $M = 150$.

Recently, the ATLAS Collaboration presented the results that a narrow resonance with SM Z couplings to fermions is excluded at 95% C.L. for masses less than 2.79 TeV in the dielectron channel, 2.53 TeV in the dimuon channel, and 2.90 TeV in the two channels combined [20]. And presented the limit on a Grand-Unification model based on the E_6 gauge group, a spin-2 graviton excitation from Randall–Sundrum models, etc. The same thing has also been explored by the CMS Collaboration and a sequential SM Z' resonance lighter than 2.59 TeV [21] is excluded at 95% C.L.

In order to constrain the mass of Z_H from the LRTH model, we show the observed and expected 95% C.L. exclusion limits on $\sigma(q\bar{q} \to Z_H) \times Br(Z_H \to l^+l^-)$ (where $l = e$ or μ) as a function of m_{Z_H} at the LHC in Fig. 1, where the observed and expected exclusion limits come from Ref. [20]. We have checked the production process $q\bar{q} \to Z_H$ and the decay $Z_H \to l^+l^-$, and found that our results were consistent with those in Ref. [13]. From Fig. 1, we can see that the limits on the m_{Z_H} are insensitive to M. In two cases, the m_{Z_H} are both required to be larger than 2.76 TeV, this is corresponding to the scale $f > 920$ GeV for $M = 0$ and $f > 900$ GeV for $M = 150$, which are much stronger than the constraints from the LHC Higgs data [22].

Meanwhile, there are many searches on the heavy top partners have been performed by both ATLAS [23,24] and CMS [25,26] Collaborations. The results show that T quarks with masses below 745 GeV are excluded at 95% C.L. for exclusive decays of $T \to tH$. For different decay modes of the T quark, the resulting mass limits range from 697 GeV, for $Br(T \to tZ) = 20\%$ and $Br(T \to bW) = 80\%$, to 782 GeV for $Br(T \to tZ) = 100\%$. However, the top quark partner T in the LRTH model can decay into $b\phi^+$, bW, tH, tZ and $t\phi^0$, and more than 70% of heavy top decays via $T \to b\phi^+$. The branching ratios of the other decays modes are suppressed since the relevant couplings are suppressed by at least one power of M/f. In the limit $M = 0$, the only two body decay mode is $T \to b\phi^+$ with a branching ratio of 100% [13]. Thus, the current constraint on the top partner will be relaxed in the LRTH model. In addition, we have checked that the limit of the scale $f > 900$ GeV satisfies the limit from the searches of T quark.

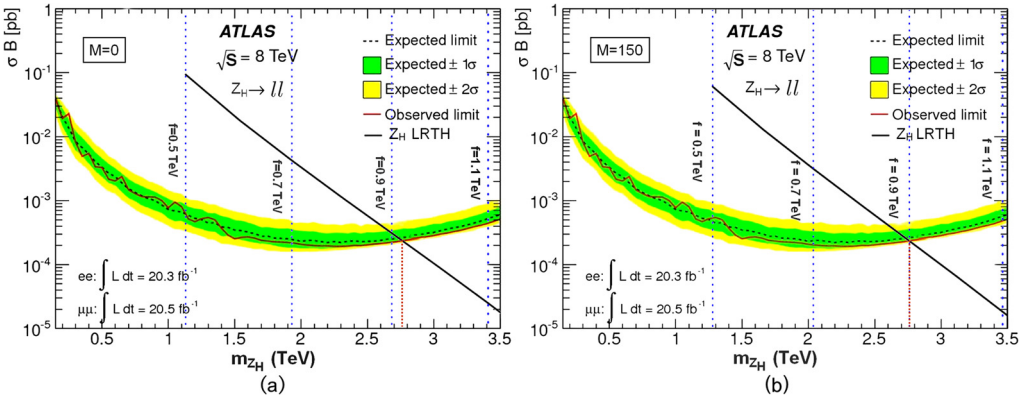

Fig. 1. $\sigma(q\bar{q} \to Z_H) \times Br(Z_H \to l^+l^-)$ (where $l = e$ or μ) as a function of m_{Z_H} at 95% C.L. observed and expected data at the LHC for $M = 0$ (a) and $M = 150$ (b) in the LRTH model.

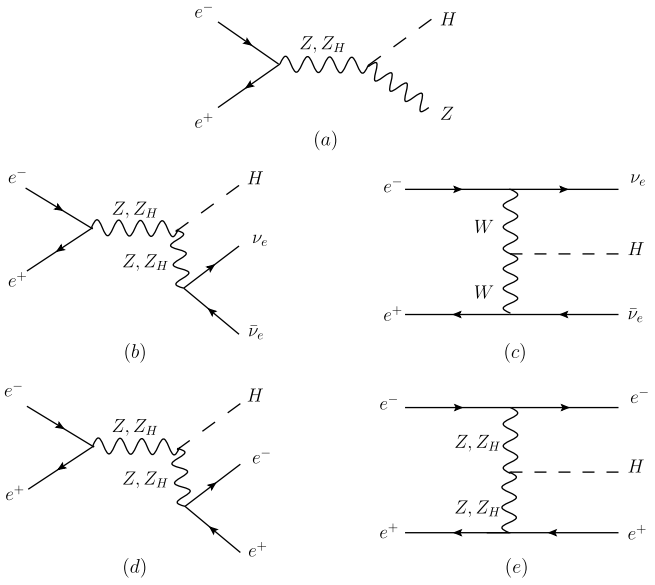

Fig. 2. Lowest-order Feynman diagrams for $e^+e^- \to ZH$ (a), $e^+e^- \to \nu_e\bar{\nu}_e H$ (b, c) and $e^+e^- \to e^+e^-H$ (d, e).

3.1. Higgs–Gauge coupling

In the LRTH model, the lowest-order Feynman diagrams of the processes $e^+e^- \to ZH$, $e^+e^- \to \nu_e\bar{\nu}_e H$ and $e^+e^- \to e^+e^-H$ are shown in Fig. 2. In comparison with the SM, we can see that the tree-level Feynman diagrams of these processes in the LRTH model receive the additional contributions arising from the heavy gauge boson Z_H.

In Fig. 3(a), we show the production cross section σ of the three processes as functions of the c.m. energy $\sqrt{s}$ for the scale $f = 1000$ GeV in the LRTH model. We can see that the Higgs strahlung process $e^+e^- \to ZH$ attains its maximum at 240–250 GeV, the cross section for ZH process is in proportion to $1/s$ and dominates the fusion process at the low energies. While the

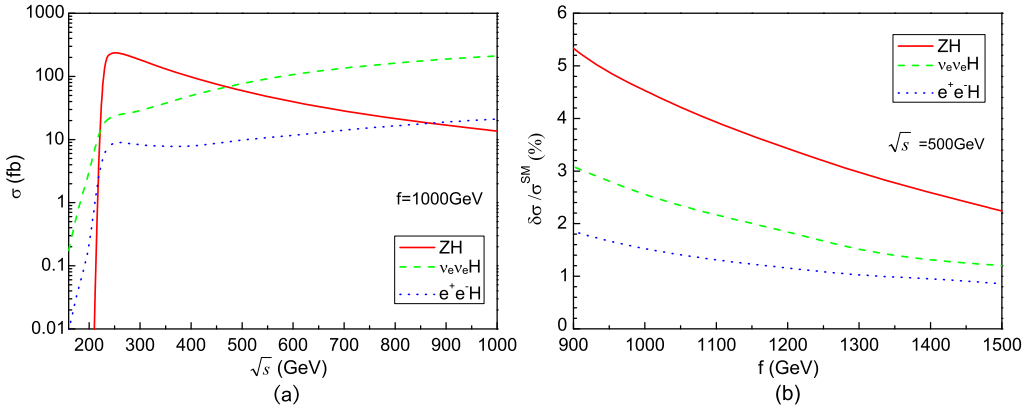

Fig. 3. The production cross section σ versus the c.m. energy $\sqrt{s}$ for $f = 1000$ GeV (a) and the relative correction $\delta\sigma/\sigma^{SM}$ versus the scale f for $\sqrt{s} = 500$ GeV (b) in the LRTH model.

cross section for $e^+e^- \to \nu_e\bar{\nu}_e H$ rises as $\log(s/m_H^2)$ and dominates at high energies. The $\nu_e\bar{\nu}_e H$ and $e^+e^- H$ production cross sections increase with the c.m. energy and can respectively take over that of the ZH process at $\sqrt{s} \geq 500$ GeV and $\sqrt{s} \geq 900$ GeV, where the cross section for the process $e^+e^- H$ is suppressed by an order of magnitude compared with the process $\nu_e\bar{\nu}_e H$.

In Fig. 3(b), we show the relative correction $\delta\sigma/\sigma^{SM}$ of the three production channels as functions of the scale f for $\sqrt{s} = 500$ GeV, respectively, where $\delta\sigma$ is defined as $\delta\sigma = \sigma^{LRTH} - \sigma^{SM}$. We can see that the values of the relative corrections decrease with the scale f increasing, which indicates that the effects of the LRTH model will decouple at the high scale f. In the same parameter space, the three curves also demonstrate the process $e^+e^- \to ZH$ has the largest relative correction, which can maximally reach 5.3% when the scale f is as low as 900 GeV.

For the process $e^+e^- \to ZH$, the 250 (500) GeV run of the ILC can measure the cross section to a relative accuracy of 2.5 (3.0)% at 250 (500) fb^{-1} [27,28]. In addition, an even more remarkable precision of 0.4% may be achieved at the recently proposed Triple-Large Electron–Positron Collider (TLEP) [29], which is a new circular e^+e^- collider operated at $\sqrt{s} = 240$ GeV with 10^4 fb^{-1} integrated luminosity. For the process $e^+e^- \to \nu_e\bar{\nu}_e H$, the ILC can measure this cross section times the branching fraction to $b\bar{b}$ to a statistical accuracy of about 0.6% at 500 GeV with an integrated luminosity of 500 fb^{-1} [27,28]. For the process $e^+e^- \to e^+e^- H$, we can see that the relative correction to the cross section of this process is very small in the LRTH model. Meanwhile, such a process is dominated by the huge SM backgrounds at the ILC. So we can conclude that it is not promising to observe the LRTH effects through $e^+e^- \to e^+e^- H$, as a comparison with $e^+e^- \to ZH$ at the ILC.

3.2. Top quark Yukawa coupling

The relevant tree-level Feynman diagrams of the process $e^+e^- \to t\bar{t}H$ in the LRTH model are shown in Fig. 4. Comparing with the SM, we can see that there are additional diagrams mediated by the heavy gauge boson Z_H, the heavy T-quark and the pseudo-scalar ϕ_0 in the LRTH model. Although a contribution can also come from the pseudo-scalar ϕ_0, such a contribution is relatively small since the $\phi_0 t\bar{t}$ coupling is suppressed by the factor (M^4/f^4).

In Fig. 5(a), we show the production cross section σ as functions of the c.m. energy $\sqrt{s}$ in the LRTH model. We take $f = 1000$ GeV and $M = 0$, 150 GeV as examples. Since the process

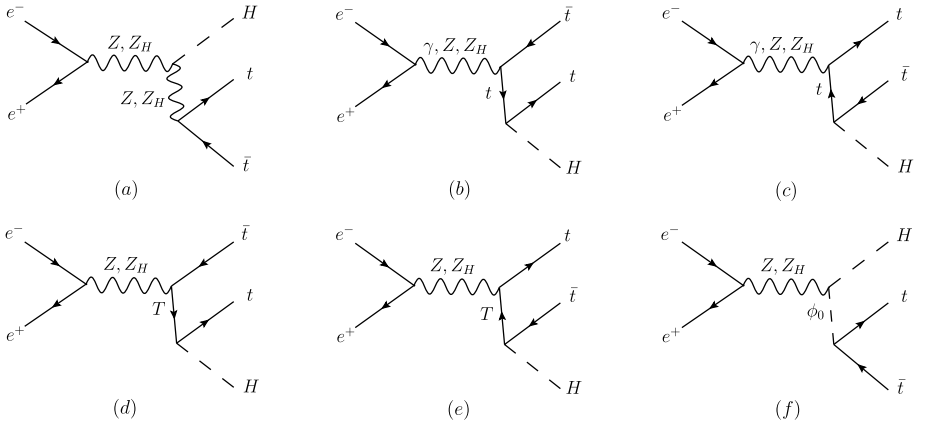

Fig. 4. Lowest-order Feynman diagrams for $e^+e^- \to t\bar{t}H$.

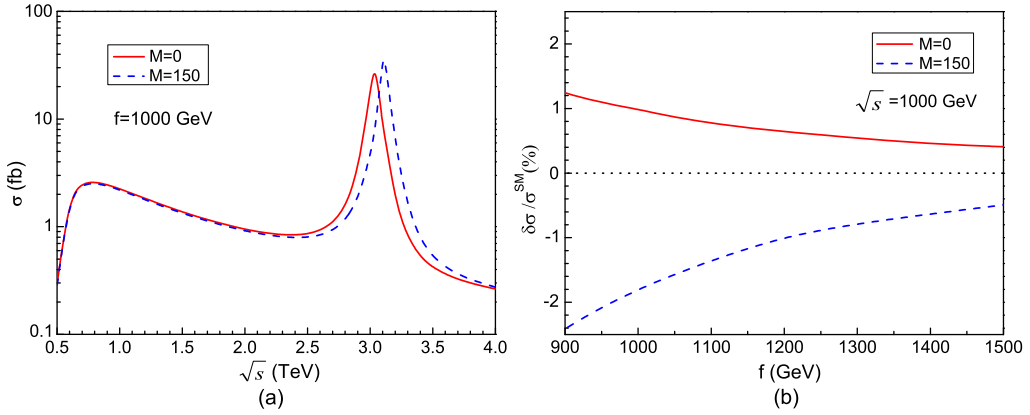

Fig. 5. The production cross section σ versus the c.m. energy $\sqrt{s}$ (a) and the relative correction $\delta\sigma/\sigma^{SM}$ versus the scale f for $\sqrt{s} = 1000$ GeV (b) in the LRTH model.

proceeds mainly through the s-channel, we can see that the cross section resonance emerges when m_{Z_H} approaches the $\sqrt{s}$. For the same scale f, the resonance peak for case $M = 0$ is smaller than that for case $M = 150$ GeV. However, the detection for such resonance effect is beyond the reach of the ILC, this could be accessed later by a multi-TEV e^+e^- collider [30]. In Fig. 5(b), we show the relative correction $\delta\sigma/\sigma^{SM}$ of the process $e^+e^- \to t\bar{t}H$ as functions of the scale f for $M = 0$, 150 GeV at the ILC. We can see that the deviation is positive for $M = 0$ and the deviation is negative for $M = 150$ GeV. When the scale f ranges from 900 GeV to 1500 GeV, the value of relative correction is less than 2.4%.

At the ILC, the 10% accuracy expected at $\sqrt{s} = 500$ GeV can be significantly improved by the data taken at 1000 GeV due to the larger cross section and the less background from $e^+e^- \to t\bar{t}$. Fast simulations at $\sqrt{s} = 800$ GeV showed that we would be able to determine the top Yukawa coupling to 6% for $m_H = 120$ GeV, given an integrated luminosity of 1000 fb^{-1} and residual background uncertainty of 5% [31]. Full simulations just recently completed by SiD and ILD showed that the top Yukawa coupling could indeed be measured to a statistical precision of 4.3%

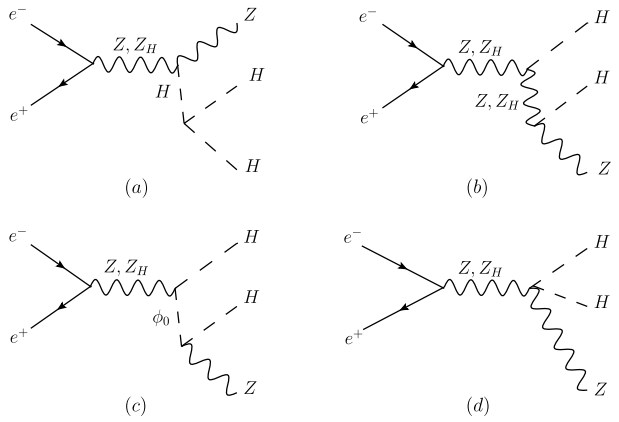

Fig. 6. Lowest-order Feynman diagrams for $e^+e^- \to ZHH$.

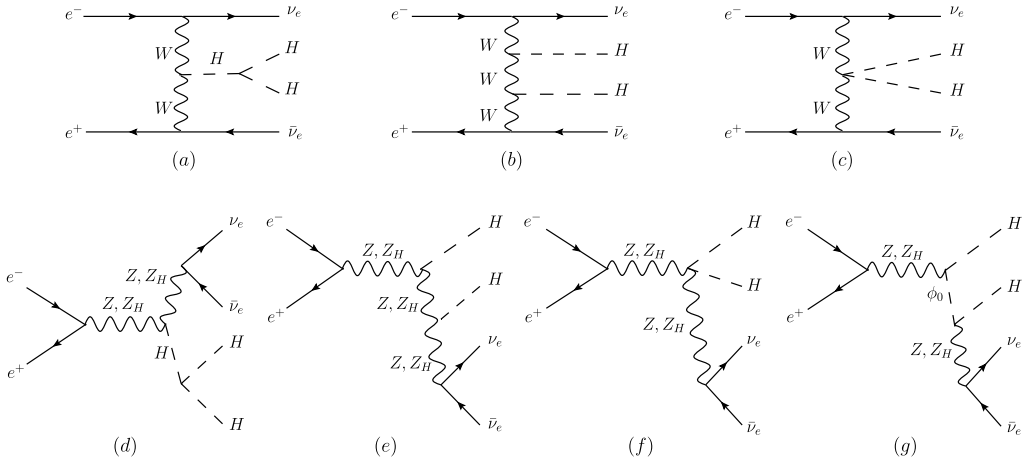

Fig. 7. Lowest-order Feynman diagrams for $e^+e^- \to \nu_e\bar{\nu}_e HH$.

for $m_H = 125$ GeV with $\sqrt{s} = 1000$ GeV and the integrated luminosity of 1000 fb^{-1} [32]. By this token, we can see that the $t\bar{t}H$ production channel will be hard to be observed at the ILC.

3.3. Higgs self-coupling

In e^+e^- collisions, the main triple Higgs boson coupling can be studied through the production channels of double Higgs-strahlung off Z bosons ($e^+e^- \to ZHH$, for $\sqrt{s} = 500$ GeV) and double Higgs fusion ($e^+e^- \to \nu_e\bar{\nu}_e HH$, for $\sqrt{s} \geq 1$ TeV). In the LRTH model, the relevant Feynman diagrams are shown in Fig. 6 and Fig. 7, respectively. In Fig. 8, we show the cross sections of the $e^+e^- \to ZHH$ and $e^+e^- \to \nu_e\bar{\nu}_e HH$ as functions of $\sqrt{s}$ in the SM and the LRTH model for the scale $f = 1000$ GeV. We can see that the cross section for the former process dominates at the low energies, while that for the latter process dominates at high energies, and they have a similar trend in the SM and the LRTH model. Since the Higgs self-coupling in the LRTH model is quite different from the SM, the values of cross sections in the LRTH model are much

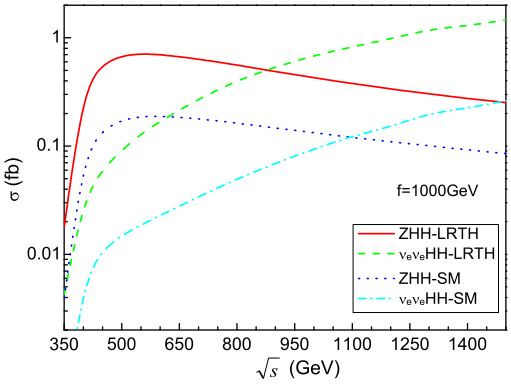

Fig. 8. The double Higgs production cross section σ versus the c.m. energy $\sqrt{s}$ for $f = 1000$ GeV in the LRTH model.

larger than the SM. The recent studies suggest that a precision of 50% for the HHH coupling can be obtained through $pp \to HH \to bb\gamma\gamma$ at the HL-LHC with an integrated luminosity of 3000 fb^{-1} [33,34], and may be further improved to be around 13% at the ILC with collision energy up to 1 TeV [33]. So, the effects of the LRTH model on these two processes should be observed at the ILC.

4. Higgs decay in the LRTH model

In order to provide more information for probing the LRTH model, we also give the effect on the Higgs decay. In the LRTH model, the major decay modes of the Higgs boson are $h \to f\bar{f}(f = b, c, \tau)$, $VV^*(V = W, Z)$, gg, $\gamma\gamma$, where W^*/Z^* denoting the off-shell charged or neutral electroweak gauge bosons. For $h \to gg$ decay, the LRTH model can give corrections via the coupling $ht\bar{t}$ and the heavy top quark loops. For $h \to \gamma\gamma$ decay, the T-quark, W_H boson and $\phi^{\pm}$ boson loops can provide the additional contributions simultaneously. By contrast, other decay models are less affected by the LRTH effect. In our calculations, the corresponding expressions of decay widths can be found in Refs. [22,35], the relative correction of the decay branching ratio is defined by

$$R = (BR^{LRTH} - BR^{SM})/BR^{SM} \tag{16}$$

In Fig. 9, we show the relative correction R as functions of the scale f for $M = 0, 150$ GeV in the LRTH model. We can see that the deviation from the SM prediction for $h \to gg$ and $h \to \gamma\gamma$ decay models decrease and finally reduce to the SM results with the increasing f. The value of relative correction R for $M = 150$ is larger than $M = 0$ and the correction R_{gg} can reach -8.9%. The expected accuracies at the ILC for the branching ratios of $h \to gg$ are 4.0% (2.9%) for $\sqrt{s} = 500$ (1000) GeV [27], so that the decay mode of $h \to gg$ might be detected.

5. Conclusion

In this paper, we investigated the three types of Higgs bosons production processes at e^+e^- colliders under the current LHC constraints as follows: (i) For the Higgs–Gauge coupling production, we studied the processes $e^+e^- \to ZH$, $e^+e^- \to \nu_e\bar{\nu}_e H$ and $e^+e^- \to e^+e^-H$. In the allowed parameter space, we found that the processes $e^+e^- \to ZH$ and $e^+e^- \to \nu_e\bar{\nu}_e H$ might

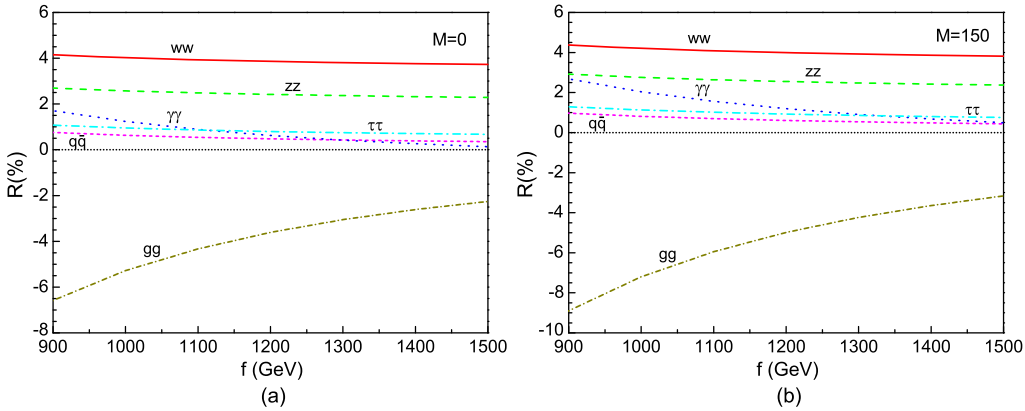

Fig. 9. The relative correction R as a function of the scale f for $M = 0$, 150 GeV in the LRTH model, respectively.

approach the observable threshold of the ILC. (ii) For the top quark Yukawa coupling production process $e^+e^- \to t\bar{t}H$, we found that the deviation of the cross section from the SM prediction is lower than 2% in a large part of allowed parameter space so that the effect will be difficult to be observed at the ILC. (iii) For the Higgs self-coupling production, we studied the processes $e^+e^- \to ZHH$ and $e^+e^- \to \nu_e\bar{\nu}_e HH$. We found that the cross sections can be enhanced greatly compared to the SM predictions and these effects may be observable at the ILC. Besides, we also investigated the impact of the LRTH model on the Higgs decay and found that the decay $h \to gg$ had an obvious deviation from the SM prediction.

Acknowledgements

This work is supported by the Joint Funds of the National Natural Science Foundation of China under Grant No. U1404113, by the Science and Technology Department of Henan province with Grant No.142300410043, by the National Natural Science Foundation of China under Grant Nos. 11405047, 11305049, and by the China Postdoctoral Science Foundation under Grant No. 2014M561987.

References

[1] G. Aad, et al., ATLAS Collaboration, Phys. Lett. B 716 (2012) 1, arXiv:1207.7214 [hep-ex].
[2] S. Chatrchyan, et al., CMS Collaboration, Phys. Lett. B 716 (2012) 30, arXiv:1207.7235 [hep-ex].
[3] ATLAS Collaboration, ATLAS-CONF-2013-040;
ATLAS Collaboration, Phys. Lett. B 726 (2013) 120, arXiv:1307.1432 [hep-ex].
[4] S. Chatrchyan, et al., CMS Collaboration, Phys. Rev. Lett. 110 (2013) 081803, arXiv:1212.6639 [hep-ex].
[5] H. Baer, et al., arXiv:1306.6352 [hep-ph].
[6] See examples: Bernd A. Kniehl, Int. J. Mod. Phys. A 17 (2002) 1457, arXiv:hep-ph/0112023;
F. Jegerlehner, O. Tarasov, Nucl. Phys. Proc. Suppl. 116 (2003) 83, arXiv:hep-ph/0212004;
G. Belanger, et al., Phys. Lett. B 559 (2003) 252, arXiv:hep-ph/0212261;
G. Belanger, et al., Nucl. Phys. Proc. Suppl. 116 (2003) 353, arXiv:hep-ph/0211268;
F. Boudjema, et al., Phys. Lett. B 600 (2004) 65, arXiv:hep-ph/0407065;
A. Denner, et al., Phys. Lett. B 560 (2003) 196, arXiv:hep-ph/0301189;
A. Denner, et al., Nucl. Phys. B 660 (2003) 289, arXiv:hep-ph/0302198.
[7] H. Eberl, W. Majerotto, V.C. Spanos, Phys. Lett. B 538 (2002) 353, arXiv:hep-ph/0204280;
H. Eberl, W. Majerotto, V.C. Spanos, Nucl. Phys. B 657 (2003) 378, arXiv:hep-ph/0210038;

T. Hahn, S. Heinemeyer, G. Weiglein, Nucl. Phys. B 652 (2003) 229, arXiv:hep-ph/0211204;
T. Hahn, S. Heinemeyer, G. Weiglein, Nucl. Phys. Proc. Suppl. 116 (2003) 336, arXiv:hep-ph/0211384;
J.J. Cao, et al., arXiv:1410.1018 [hep-ph].
[8] C.-X. Yue, S.Z. Wang, D.Q. Yu, Phys. Rev. D 68 (2003) 115004, arXiv:hep-ph/0309113;
C.-X. Yue, W. Wang, Z.J. Zong, F. Zhang, Eur. Phys. J. C 42 (2005) 331, arXiv:hep-ph/0504253;
X.L. Wang, et al., Eur. Phys. J. C 49 (2007) 593, arXiv:hep-ph/0607131;
S.L. Hu, N. Liu, J. Ren, L. Wu, J. Phys. G 41 (2014) 125004;
N. Liu, et al., J. High Energy Phys. 1404 (2014) 189, arXiv:1311.6971 [hep-ph];
B.F. Yang, J.Z. Han, S.H. Zhou, N. Liu, J. Phys. G 41 (2014) 075009, arXiv:1401.0289 [hep-ph].
[9] L. Wang, W.Y. Wang, J.M. Yang, H.J. Zhang, Phys. Rev. D 75 (2007) 074006, arXiv:hep-ph/0609200;
J.F. Shen, J. Cao, L.B. Yan, Europhys. Lett. 91 (2010) 51001;
N. Liu, et al., J. High Energy Phys. 1501 (2015) 008, arXiv:1408.4191 [hep-ph];
N. Liu, et al., J. High Energy Phys. 1301 (2013) 161, arXiv:1208.3413 [hep-ph];
J.J. Cao, et al., arXiv:1410.1018 [hep-ph];
A. Kobakhidze, et al., J. High Energy Phys. 1410 (2014) 100, arXiv:1406.1961 [hep-ph];
B.F. Yang, Z.Y. Liu, N. Liu, J.Z. Han, Eur. Phys. J. C 74 (2014) 3203, arXiv:1408.4295 [hep-ph];
B.F. Yang, J.Z. Han, N. Liu, arXiv:1412.2927 [hep-ph];
L. Wu, J. High Energy Phys. 1502 (2015) 061, arXiv:1407.6113 [hep-ph].
[10] Z. Chacko, H.-S. Goh, R. Harnik, Phys. Rev. Lett. 96 (2006) 231802, arXiv:hep-ph/0506256;
Z. Chacko, Y. Nomura, M. Papucci, G. Perez, J. High Energy Phys. 0601 (2006) 126, arXiv:hep-ph/0510273;
A. Falkowski, S. Pokorski, M. Schmaltz, Phys. Rev. D 74 (2006) 035003, arXiv:hep-ph/0604066;
R. Foot, R.R. Volkas, Phys. Lett. B 645 (2007) 75, arXiv:hep-ph/0610013.
[11] Z. Chacko, H.-S. Goh, R. Harnik, J. High Energy Phys. 0601 (2006) 108, arXiv:hep-ph/0512088.
[12] N. Arkani-Hamed, A.G. Cohen, E. Katz, A.E. Nelson, J. High Energy Phys. 0207 (2002) 034, arXiv:hep-ph/0206021;
I. Low, W. Skiba, D. Smith, Phys. Rev. D 66 (2002) 072001, arXiv:hep-ph/0207243;
D.E. Kaplan, M. Schmaltz, J. High Energy Phys. 0310 (2003) 039, arXiv:hep-ph/0302049;
W. Skiba, J. Terning, Phys. Rev. D 68 (2003) 075001, arXiv:hep-ph/0305302;
S. Chang, J. High Energy Phys. 0312 (2003) 057, arXiv:hep-ph/0306034;
T. Han, H.E. Logan, B. McElrath, L.T. Wang, Phys. Rev. D 67 (2003) 095004, arXiv:hep-ph/0208067.
[13] H.-S. Goh, S. Su, Phys. Rev. D 75 (2007) 075010, arXiv:hep-ph/0611015.
[14] E.M. Dolle, S. Su, Phys. Rev. D 77 (2008) 075013, arXiv:0712.1234 [hep-ph].
[15] H.-S. Goh, C.A. Krenke, Phys. Rev. D 76 (2007) 115018, arXiv:0707.3650 [hep-ph];
H.-S. Goh, C.A. Krenke, Phys. Rev. D 81 (2010) 055008, arXiv:0911.5567 [hep-ph];
A. Abada, I. Hidalgo, Phys. Rev. D 77 (2008) 113013, arXiv:0711.1238 [hep-ph].
[16] Y.-B. Liu, Phys. Lett. B 698 (2011) 157;
Y.-B. Liu, Z.-J. Xiao, J. High Energy Phys. 1402 (2014) 128, arXiv:1312.4004 [hep-ph].
[17] W. Ma, C.-X. Yue, Y.-Z. Wang, Phys. Rev. D 79 (2009) 095010, arXiv:0905.0597 [hep-ph];
L. Wang, L. Wu, J.M. Yang, Phys. Rev. D 85 (2012) 075017, arXiv:1111.4771 [hep-ph];
J.Z. Han, B.F. Yang, X.T. Zhang, Europhys. Lett. 105 (2014) 31001, arXiv:1401.3594 [hep-ph];
J.H. Han, B.Z. Li, Commun. Theor. Phys. 60 (2013) 205.
[18] S. Su, H.S. Goh, E. Dolle, http://www.physics.arizona.edu/~shufang/twinhiggs.html.
[19] J. Beringer, et al., Particle Data Group, Phys. Rev. D 86 (2012) 010001, and 2013 partial update for the 2014 edition.
[20] G. Aad, et al., ATLAS Collaboration, Phys. Rev. D 90 (2014) 052005, arXiv:1405.4123 [hep-ex].
[21] S. Chatrchyan, et al., CMS Collaboration, Phys. Lett. B 720 (2013) 63, arXiv:1212.6175 [hep-ex].
[22] Y.-B. Liu, S. Cheng, Z.-J. Xiao, Phys. Rev. D 89 (2014) 015013, arXiv:1311.0183 [hep-ph].
[23] ATLAS Collaboration, ATLAS-CONF-2013-018;
G. Aad, et al., ATLAS Collaboration, J. High Energy Phys. 1211 (2012) 094, arXiv:1209.4186 [hep-ex].
[24] G. Aad, et al., ATLAS Collaboration, Phys. Lett. B 712 (2012) 22, arXiv:1112.5755 [hep-ex];
G. Aad, et al., ATLAS Collaboration, Phys. Rev. D 86 (2012) 012007, arXiv:1202.3389 [hep-ex].
[25] S. Chatrchyan, et al., CMS Collaboration, J. High Energy Phys. 1301 (2013) 154, arXiv:1210.7471 [hep-ex].
[26] S. Chatrchyan, et al., CMS Collaboration, Phys. Lett. B 718 (2012) 307, arXiv:1209.0471 [hep-ph].
[27] D.M. Asner, T. Barklow, C. Calancha, et al., arXiv:1310.0763 [hep-ph].
[28] H. Baer, et al., The International Linear Collider Technical Design Report, Volume 2: Physics, arXiv:1306.6352 [hep-ph].
[29] M. Koratzinos, et al., arXiv:1305.6498 [physics.acc-ph];

M. Bicer, et al., TLEP Design Study Working Group Collaboration, J. High Energy Phys. 1401 (2014) 164, arXiv:1308.6176 [hep-ex].
[30] H. Abramowicz, et al., CLIC Detector and Physics Study Collaboration, arXiv:1307.5288 [hep-ph].
[31] A. Gay, Eur. Phys. J. C 49 (2007) 489, arXiv:hep-ph/0604034.
[32] H. Baer, et al., The International Linear Collider Technical Design Report, Volume 4: Detectors, arXiv:1306.6329 [physics.ins-det].
[33] S. Dawson, et al., arXiv:1310.8361 [hep-ex];
T. Han, Z. Liu, J. Sayre, arXiv:1311.7155 [hep-ph];
M.E. Peskin, arXiv:1312.4974 [hep-ph];
P. Bechtle, et al., arXiv:1403.1582 [hep-ph].
[34] F. Goertz, A. Papaefstathiou, L.L. Yang, J. Zurita, J. High Energy Phys. 1306 (2013) 016, arXiv:1301.3492 [hep-ph];
R.S. Gupta, H. Rzehak, J.D. Wells, Phys. Rev. D 88 (2013) 055024, arXiv:1305.6397 [hep-ph].
[35] A. Djouadi, Phys. Rep. 457 (2008) 1, arXiv:hep-ph/0503172.